JACS
JOURNAL OF THE AMERICAN CHEMICAL SOCIETY
Article
pubs.acs.org/JACS

Superoxide Reaction with Tyrosyl Radicals Generates *para*-Hydroperoxy and *para*-Hydroxy Derivatives of Tyrosine

Matías N. Möller,[†,‡] Duane M. Hatch,[†] Hye-Young H. Kim,[†] and Ned A. Porter*[,†]

[†]Department of Chemistry and Vanderbilt Institute of Chemical Biology, Vanderbilt University, Nashville, Tennessee 37235, United States

[‡] Instituto de Química Biológica, Facultad de Ciencias, and Center for Free Radical and Biomedical Research, Universidad de la República, Montevideo, Uruguay

Supporting Information

ABSTRACT: Tyrosine-derived hydroperoxides are formed in peptides and proteins exposed to enzymatic or cellular sources of superoxide and oxidizing species as a result of the nearly diffusion-limited reaction between tyrosyl radical and superoxide. However, the structure of these products, which informs their reactivity in biology, has not been unequivocally established. We report here the complete characterization of the products formed in the addition of superoxide, generated from xanthine oxidase, to several peptide-derived tyrosyl radicals, formed from horseradish peroxidase. RP-HPLC, LC-MS, and NMR experiments indicate that the primary stable products of superoxide addition to tyrosyl radical are *para*-hydroperoxide derivatives (*para* relative to the position of the OH in tyrosine) that can be reduced to the corresponding *para*-alcohol. In the case of glycyl-tyrosine, a stable 3-(1-hydroperoxy-4-oxocyclohexa-2,5-dien-1-yl)-L-alanine was formed. In tyrosyl-glycine and Leu-enkephalin, which have N-terminal tyrosines, bicyclic indolic *para*-hydroperoxide derivatives were formed ((2*S*,3a*R*,7a*R*)-3a-hydroperoxy-6-oxo-2,3,3a,6,7,7a-hexahydro-1H-indole-2-carboxylic acid) by the conjugate addition of the free amine to the cyclohexadienone. It was also found that significant amounts of the *para*-OH derivative were generated from the hydroxyl radical, formed on exposure of tyrosine-containing peptides to Fenton conditions. The *para*-OOH and *para*-OH derivatives are much more reactive than other tyrosine oxidation products and may play important roles in physiology and disease.

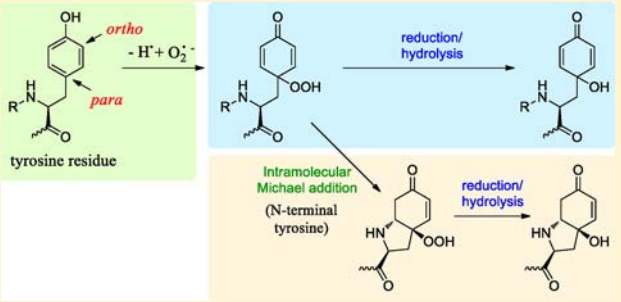

INTRODUCTION

Oxidation of tyrosine by free radicals and other reactive species occurs under physiological conditions and is usually augmented in many pathologies as a consequence of increased production of reactive species.[1−3] Reported oxidative modifications of tyrosine generally involve substitutions at the *ortho* position of the tyrosine phenol (relative to the OH), such as the case for *o*-nitrotyrosine, *o*,*o*′-dityrosine, and *o*-chlorotyrosine (Figure 1).[1−7] These stable products are thermodynamically favored by re-aromatization of the phenolic ring subsequent to substitution. The *para* position is usually considered much less reactive because of steric hindrance toward substitution along with the loss of the rearomatization stabilization. However, there are some reactions that modify tyrosine in the *para* position, including the reaction between tyrosyl radical and lipid peroxyl radicals[8] and the reaction between tyrosine and singlet oxygen.[9,10]

Superoxide addition to tyrosyl radical was proposed to occur at both *ortho* and *para* positions,[11] but there is still some debate about the structure of the products formed from this reaction. In the first study of this reaction, Jin, Leitich, and von Sonntag isolated two products, a mixture of diasteroisomers of a bicyclic *p*-hydroxy derivative of tyrosine (assigned to (2*S*,3a*R*,7a*S*)- and (2*S*,3a*S*,7a*R*)-3a-hydroxy-6-oxo-2,3,3a,6,7,7a-hexa-hydro-1H-indole-2-carboxylic acids, HOHICA, Figure 1).[11] These products

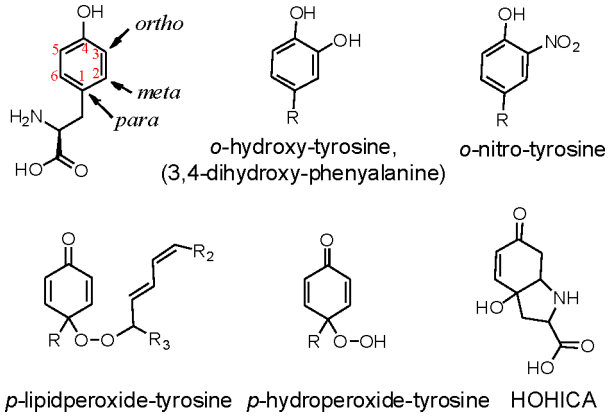

Figure 1. Tyrosine structure showing the different ring positions and different products of tyrosine oxidation involving modifications at the *ortho* and *para* positions.

Received: July 23, 2012
Published: September 18, 2012

   dx.doi.org/10.1021/ja307215z | J. Am. Chem. Soc. 2012, 134, 16773−16780

Scheme 1

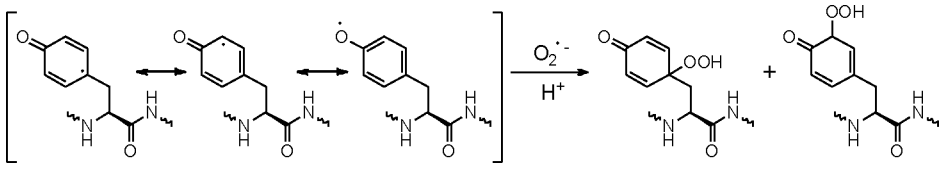

were proposed to derive from intermediate hydroperoxides formed at both *ortho* and *para* positions that could undergo intramolecular conjugate addition by the free amine followed by hydrolysis.[11]

More recent studies have observed the formation of tyrosine hydroperoxides from the addition of superoxide to tyrosyl radical in many tyrosine-containing peptides[12−14] and in myoglobin[15] using LC-MS and hydroperoxide assays. Some of these studies included xanthine oxidase (XO) as an enzymatic source of superoxide and hydrogen peroxide[12,13,15] and horseradish peroxidase (HRP) to catalyze the formation of tyrosyl radicals.[12,13] Interestingly, the same products were observed after exposing the peptides to activated neutrophils,[14] supporting the plausibility of these reactions *in vivo*. Characterization by mass spectrometry confirmed that hydroperoxide and alcohol derivatives were formed in the tyrosine residues, but the structures were not unambiguously established.[12−16] Nonetheless, mechanisms and structures show products from exclusive addition of superoxide to the *ortho* position, see Scheme 1.[12,14−18]

Recent studies in our laboratory demonstrated that lipid peroxyl radicals undergo reaction exclusively at the tyrosyl *para* position, an observation that led us to compare this result with the *ortho*−*para* selectivity of tyrosyl-superoxide adduction.[8]

We report here that tyrosine-containing peptides oxidized with xanthine oxidase−horseradish peroxidase give *para*-coupled adducts as the major products. The formation of *para*-substituted cyclohexadienones from tyrosine oxidation is of interest due to its general novelty as well as to challenge the "steric hindrance" and "rearomatization stabilization" argument invoked to explain the reactions of other reactive species with tyrosine. Furthermore, the cyclohexadienone product is a bifunctional electrophile that potentially reacts with one or two nucleophiles to generate novel Michael-type adducts to promote protein covalent cross-links and trigger electrophile response signaling events. The hydroperoxide and alcohol−peptide derivatives of this reaction were examined by LC-MS and HPLC-UV and compared to various oxidative systems. Authentic standards were prepared that allowed the complete structural characterization by NMR as well as quantification of the products formed.

EXPERIMENTAL SECTION

Materials. Glycyl-tyrosine was from TCI (Portland, OR), tyrosyl-glycine was from Bachem (Torrance, CA), and Leu-enkephalin (Leu-enk) was from American Peptide Company (Sunnyvale, CA). Mushroom tyrosinase was from Pfaltz & Bauer (Waterbury, CT), xanthine oxidase (XO, grade I), horseradish peroxidase (HRP, Type VI), superoxide dismutase from bovine erythrocytes (SOD), and dimethyl sulfide (DMS) were from Sigma (St Louis, MO). Tyrosine-containing peptides were quantified by UV spectrophotometry, ε_{275} = 1470 M^{-1} cm^{-1}.[19]

Oxidation of Peptides with Xanthine Oxidase and Horseradish Peroxidase. Oxidation of tyrosine-containing peptides with this system was based on the work of Winterbourn et al.[12,13] Briefly, to 200 μM peptide in 50 mM phosphate buffer, 0.1 mM DTPA at pH 7.4, was added 140 nM HRP and flushed with oxygen for 3 min. Then, 1 mM acetaldehyde was added, and then XO was added, mixed, and left to react for 30 min at room temperature (23 °C), with mechanical agitation and protected from light. Each condition was done in triplicate. The production of superoxide by XO was measured previous to the assay by cytochrome c reduction[15] and then was added to the reaction mixture the quantity necessary to generate 3.8 μM $O_2^{\bullet -}$ min^{-1}. Typical conditions involved a total 1000-fold dilution of the stock XO. In some assays, 10 μg/mL SOD was included. After 30 min, the samples were treated with catalase (10 μg/mL) for 10 min in the dark to remove remaining H_2O_2. The samples were then filtered through a 0.22 μm nylon filter (Costar) and taken to 0.2 M HCl with 4 M HCl to prevent degradation of the hydroxylation products. This sample was split into two. One was analyzed directly by HPLC, while the other was reduced with 40 mM DMS (from 2.0 M DMS in acetonitrile) for 1 h at room temperature, with mechanical agitation and protected from light.

Hydroxylation of Peptides by Hydroxyl Radical. Oxidation of the peptides with H_2O_2 in the presence of Fe(II):EDTA (1:2) was performed in 5 mM sodium phosphate at pH 7.4, using 2 mM peptide and either 0.2 mM H_2O_2 and 0.2 mM Fe(II):EDTA (1:2) or 4 mM H_2O_2 and 4 mM Fe(II):EDTA (1:2). The Fe(II):EDTA (1:2) solution was prepared fresh from mixing equal volumes of 20 mM $FeSO_4$ and 40 mM EDTA (pH 7.4). After mixing with H_2O_2, the reaction was allowed to proceed for 5 min, and then the sample was taken to 0.2 M HCl using 4 M HCl and kept on ice to prevent degradation of the hydroxylated products. For LC-MS analysis, the samples were concentrated 5−10-fold in a speedvac at room temperature (1 h).

Synthesis of *o*-OH Derivatives. *o*-OH derivatives of the tyrosine-containing peptides were synthesized using mushroom tyrosinase in the presence of ascorbate to prevent further oxidation, as described.[20] *o*-OH-tyrosine-containing peptides were isolated by preparative HPLC (see HPLC conditions below). The peptides were confirmed by UV, MS, and NMR and quantified by UV spectrophotometry, ε_{280} = 2700 M^{-1} cm^{-1}.[20]

Synthesis of *p*-Hydroperoxide- and *p*-Hydroxytyrosine Derivatives. *p*-OOH derivatives were prepared by singlet oxygen ($^1O_2$, molecular oxygen in its $^1\Delta_g$ state) mediated oxidation of the peptide. A solution of 10 mM peptide and 30 μM methylene blue in D_2O at pH 7 was exposed to visible light (two 200 W white light bulbs) with constant oxygen bubbling and stirring in an ice bath for 1 h. Under these conditions, the *p*-OOH was formed as a major product, while some of the *p*-OH derivative was also observed. No *o*-OH derivative or dimers were observed under these conditions. The *p*-OH derivative was obtained by reduction with 0.1 M DMS in the presence of acetonitrile (30% of the total volume) for 1 h at room temperature and protected from light. The reaction mixture was then dried by rotary evaporation, redissolved in water, and purified by preparative HPLC. The purified *p*-OH derivatives were characterized by MS and NMR.

HPLC Conditions. HPLC experiments were done on an Alliance HPLC equipped with diode array UV detection (Waters, Milford, MA). Preparative HPLC was done using a Discovery C18 column (250 × 21.2 mm, 5 μm, Supelco), while analytical HPLC was done using a Microsorb-MV 100-5 C18 column (250 × 4.6 mm, 5 μm, Varian). The mobile phase consisted of 0.1% trifluoroacetic acid in (A) water and (B) acetonitrile. HPLC condition 1: to separate small peptides, 100% A was used for 10 min, and then a gradient with B was set. HPLC condition 2: Leu-enk derivatives were separated starting with 85% A for 10 min and then increasing B with time. The products

dx.doi.org/10.1021/ja307215z | J. Am. Chem. Soc. 2012, 134, 16773−16780

from the oxidation of peptides by XO and HRP were identified by comparing the retention times and UV spectra with $^1O_2$-oxidized peptide ± DMS, with NMR quantified *p*-OH derivative + starting peptide, with isolated *o*-OH derivatives (synthesized using tyrosinase), and with starting peptide. Response factors for the starting peptide and the isolated *o*-OH derivative were determined by measuring the area of the peaks at 280 nm of UV spectrophotometry quantified samples. The response factor for the *p*-OH derivatives was obtained as follows: A known amount of the unmodified peptide was added to the isolated *p*-OH derivative, and the relative concentrations were quantified by ^{1}H integration in NMR. This mixture was then analyzed by HPLC-UV. The concentration of unmodified peptide in this mixture was quantified, allowing for the calculation of the concentration of *p*-OH and the response factor at different wavelengths. The response factor obtained for the *p*-OH derivatives was also used to quantify the *p*-OOH derivatives because they share the same chromophore.

LC-ESI Mass Spectrometry. HPLC–MS/MS analysis was performed on a Waters Aquity UPLC system (Waters, Milford, MA) equipped with a Thermo LTQ ion trap mass spectrometer (Thermo Fisher Scientific, Waltham, MA), operating in the ESI positive ion mode. The separation was performed on a 150 × 4.6 mm Luna 3 μ C18(2) 100 Å column (Phenomenex, Torrance, CA) with solvents consisting of 1% formic acid in (A) water and (B) acetonitrile with flow rate 350 μL/min. Gradient elution of the peptides was achieved starting at 100% A for 10 min for glycyl-tyrosine (GY) and tyrosyl-glycine (YG) derivatives or at 85% A for Leu-enk. MS analysis was performed in a full scan followed by five data-dependent MS/MS scans.

NMR Spectroscopy. All reported NMR spectra were acquired using a 14.1 T Bruker magnet equipped with a Bruker DRX spectrometer operating at proton Larmor frequency of 600.13 MHz. ^{1}H spectra were acquired in 2.5 mm NMR tubes using a Bruker 5 mm cryogenically cooled NMR probe. NMR samples were prepared in D_2O, which also served as the ^{2}H lock solvent, and chemical shifts were referenced internally to HDO (4.79 ppm). ^{1}H, ^{13}C, 2D COSY, HSQC, and HMBC were obtained for all the adducts for structural assignment. The stereochemistry of some of the adducts was confirmed by nuclear Overhauser enhancement (NOE) experiments.

RESULTS

LC-MS Analysis of GY Oxidation Products. GY (**1**) was incubated with XO and HRP, and the oxidation progress was monitored by LC-MS (Figure 2). Two hydroxylated derivatives of GY at retention times 7.8 and 18 min (m/z = 255) and one hydroperoxide derivative (m/z = 271) were formed. The peak at 7.8 min (m/z = 255) had the same retention time and fragmentation pattern as that generated by $^1O_2$ (Figure 2B), which corresponded to the *p*-OH derivative of GY (**3**). The most distinct product ion was m/z = 180, which corresponded to the simultaneous loss of water and glycine (Figure 2C,c). The peak at 10.5 min (m/z = 271) has the same retention time and fragmentation pattern as that generated by $^1O_2$ (Figure 2B), and corresponded to *p*-OOH **2.** The major fragment m/z = 214 corresponded to the loss of glycine, with the two atoms of oxygen remaining attached to the tyrosine. Other fragments indicated the loss of H_2O_2 and O_2, consistent with the presence of a hydroperoxide in the tyrosine. The minor product at 18 min (m/z = 255) had the same retention time and fragmentation pattern as the main product from the reaction with hydroxyl radical (H_2O_2 + Fe(II):EDTA), which corresponded to the *o*-OH derivative of tyrosine (**4**). The fragmentation pattern of *o*-OH **4** was similar to that of GY **1**, where loss of CH_2O_2 and loss of glycine predominated. Loss of water was also observed for both molecules (Figure 2C,d). The main difference between the mass spectra of *o*-OH **4** and *p*-OH **3**, was the loss of a second molecule of water for *p*-OH **3**, a pattern that may serve as a diagnostic fragmentation for *p*-OH derivatives of tyrosine.

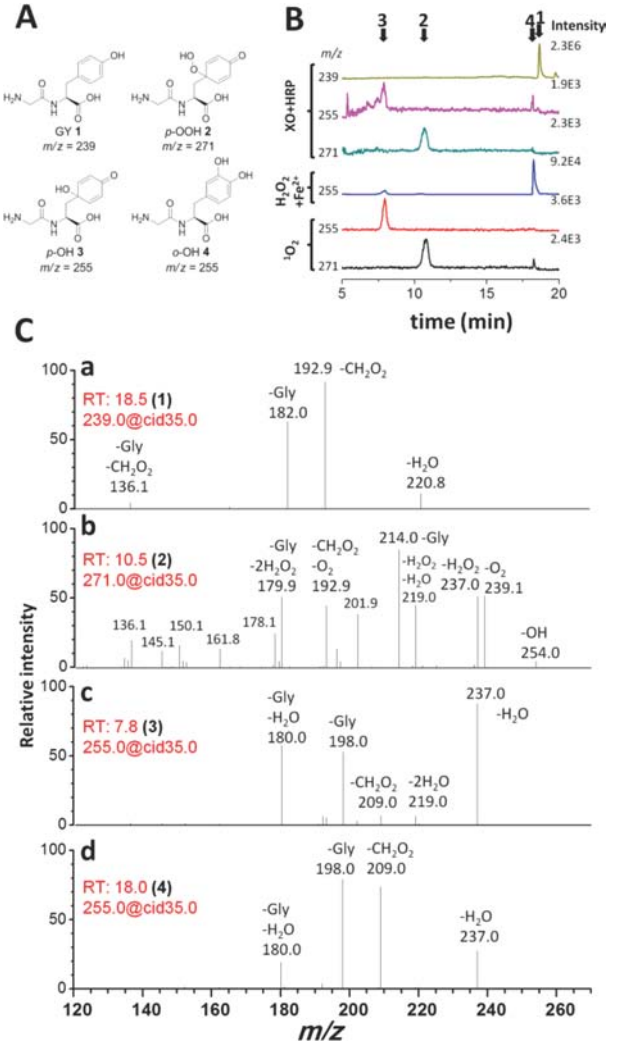

Figure 2. Oxidation of GY. (A) GY and GY-oxidation products. (B) Extracted ion chromatograms of GY hydroperoxide (m/z = 271) and the alcohol derivatives (m/z = 255) after exposure to different oxidizing systems. XO/HRP: 200 μM GY was incubated with XO and 1 mM acetaldehyde that generated 3.8 μM $O_2^{\bullet -}$/min and 140 nM HRP in 50 mM sodium phosphate, 0.1 mM DTPA pH 7.4 for 30 min at room temperature protected from light. The reaction was stopped by addition of 10 μg/mL catalase, filtration, and acidification to 0.2 M HCl and then analyzed by LC-MS. A hydroxyl radical producing system, H_2O_2 and Fe(II):EDTA, was used to produce a mixture enriched in *o*-OH **4**. The *p*-OOH **2** and *p*-OH **3** derivatives were prepared with $^1O_2$. By comparison with these products, it was concluded that the XO/HRP system produced all three *p*-OOH **2**, *p*-OH **3**, and *o*-OH **4**. (C) Product ions of GY and hydroxylated derivatives: (a) GY; (b) *p*-OOH **2**; (c) *p*-OH **3**; (d) *o*-OH **4**. *p*-OOH **2** showed a complex fragmentation involving loss of O_2 and H_2O_2, indicating the presence of a hydroperoxide group, while the fragmentation of both *p*-OH **3** and *o*-OH **4** was more similar to that of the original peptide. The most significant difference between the fragmentation of *p*-OH **3** and *o*-OH **4** is the loss of a second molecule of water by *p*-OH **3**.

NMR Structural Characterization of Products. Unambiguous structural assignments were done by NMR studies. Distinctive chemical shifts and splitting patterns of *p*-OH **3** revealed obvious differences relative to GY **1** and *o*-OH **4**. As

dx.doi.org/10.1021/ja307215z | J. Am. Chem. Soc. 2012, 134, 16773–16780

shown in Figure 3, GY **1** has symmetric aromatic protons H2 and H6 at 7.2 ppm and H3 and H5 at 6.9 ppm. Further, the

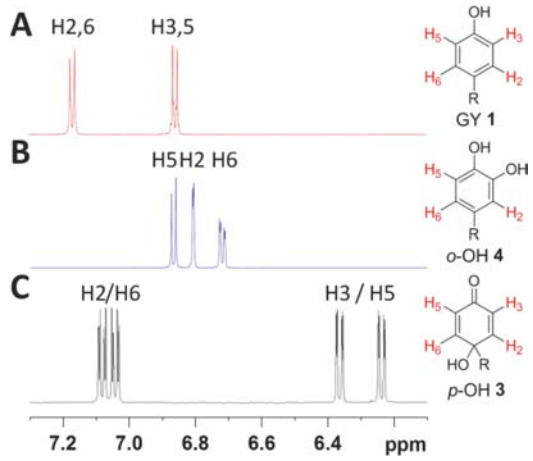

Figure 3. ^{1}H NMR spectra in the aromatic−vinylic region of GY derivatives. (A) GY **1** shows two doublets of doublets corresponding to the equivalent protons at positions 2 and 6 (7.17 ppm) and 3 and 5 (6.86 ppm). (B) *o*-OH **4** shows three nonequivalent protons at positions 5 (6.87), 2 (6.81), and 6 (6.73 ppm). (C) *p*-OH **3** shows four distinctive diastereotopic protons with one bond and long-range couplings corresponding to the positions 2/6 (7.08)/(7.04) and 3/5 (6.36)/(6.24) ppm. ^{1}H assignments were based on the distinctive chemical shifts, splitting patterns, and 2D-NMR experiments, including COSY, HSQC, and HMBC. All the spectra were acquired in D_2O at 298 K.

assignments were confirmed by HMBC to phenolic carbon at 154.1 ppm (Table S1). In contrast, all four separate peaks in the aromatic−vinylic region for *p*-OH **3** (Figure 4C) indicated that all protons are in different environments. ^{13}C shift at 188.3 ppm (Table S1) is consistent with the formation of a carbonyl,[8] and its HMBC correlations to protons H2 and H6 confirmed the *para*-substituted cyclohexadienone. Similar NMR assignments were reported for the *p*-OOH and *p*-OH cyclohexadienone derivatives of 3-(4-hydroxyphenyl)-propionic acid and of the peptide Gly-Tyr-Gly by Wright et al. [9] The *o*-OH product **4**, which was generated using mushroom tyrosinase,[20] showed an absorption peak at 280 nm in the UV and three different protons in the aromatic region in NMR that also distinctively differ from GY **1** and *p*-OH **3** but are consistent with the 3,4-dihydroxyphenylalanine structure (Figure 3).

Quantification of GY Oxidation Products with XO and HRP. The products of GY oxidation by XO and HRP were quantified by HPLC-UV. Under HPLC condition 1, *p*-OH **3** and *p*-OOH **2** eluted at 5.8 and 7.9 min, respectively, with maximal absorption at 227 nm, while *o*-OH **4** eluted at 22.2 min (Figure 4) with an absorption peak at 280 nm. The analysis shows that the products of the reaction between superoxide and tyrosyl radical were the hydroperoxide *p*-OOH **2** (1.2 μM), followed by *p*-OH **3** (0.35 μM) and *o*-OH **4** (0.2 μM) (Figure 4). After reduction with DMS, *p*-OOH **2** was converted stoichiometrically into *p*-OH **3** (1.7 μM), whereas the yield of *o*-OH **4** (0.2 μM) was not affected by DMS. We conclude that *para* addition dominates the reaction of tyrosyl and superoxide, with the *ortho* addition product being formed at about 12−15% of the *para* products.

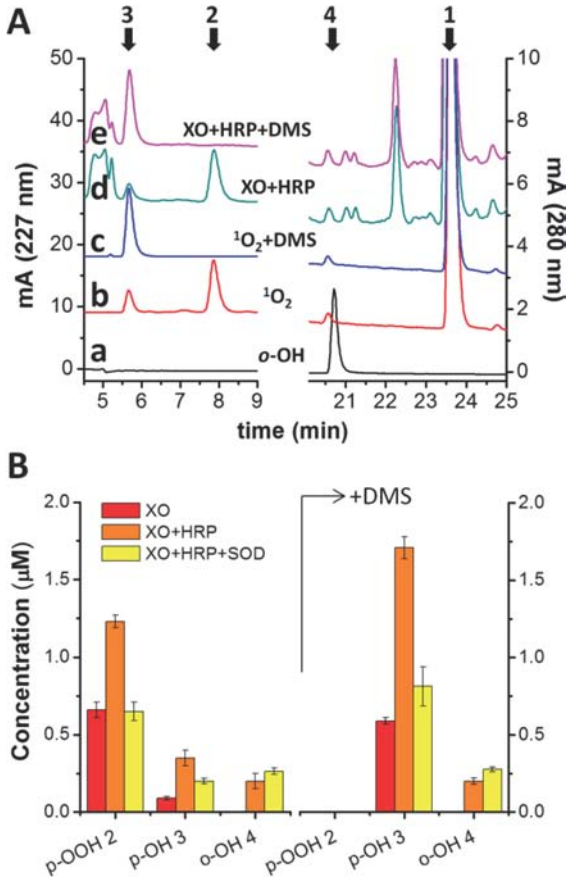

Figure 4. Quantification of the products from GY oxidation with XO and HRP. (A) HPLC separation of products of GY oxidation by XO and HRP monitored at 227 and 280 nm. (a) Authentic *o*-OH **4** produced with mushroom tyrosinase; (b) $^1O_2$-oxidized GY **1**, showing *p*-OOH **2** and *p*-OH **3**; (c) $^1O_2$-oxidized GY **1** reduced with DMS, showing *p*-OH **3** only; (d) GY **1** oxidized with XO and HRP using the conditions described in Figure 2, which generated *p*-OOH **2**, *p*-OH **3**, and *o*-OH **4**; (e) GY **1** oxidized with XO and HRP followed by DMS reduction. The *p*-OOH **2** was completely reduced to the *p*-OH **3**, while no change occurred in *o*-OH **4**. (B) Quantification of the products showed that the primary products were *p*-OOH **2**, followed by *p*-OH **3** and then *o*-OH **4**. Omission of HRP or addition of SOD to the oxidizing system led to a significant decrease in the formation of both *p*-OOH **2** and *p*-OH **3**, confirming the involvement of both superoxide and tyrosyl radical in the formation of these products. Treatment with DMS led to the complete reduction of the *p*-OOH **2** and formation of *p*-OH **3**, with no change in *o*-OH **4** levels.

The involvement of superoxide and tyrosyl radical in the generation of these products was evidenced by the significant decrease in *p*-OOH **2** in the absence of HRP or after the addition of SOD (Figure 4B). The production of *p*-OOH **2** in the absence of HRP is probably mediated by hydroperoxyl radical, the protonation product of superoxide (pK_a = 4.8), that is theoretically capable of oxidizing tyrosine.[21,22] This oxidation was very sensitive to SOD, which reduced to zero the production of *p*-OOH **2** (not shown).

LC-MS Analysis of YG Oxidation Products. Oxidation of YG with XO and HRP gave two hydroperoxides, *p*-OOH **6** and **7** (m/z = 271), and two alcohol derivatives, *p*-OH **8** and **9** (m/z = 255), of the dipeptide (Figure 5). These structures have been confirmed by comparison with standards generated using $^1O_2$ oxidation and subsequent analyses. Reduction with DMS converted both *p*-OOH **6** and **7** to the corresponding *p*-OH **8**

dx.doi.org/10.1021/ja307215z | J. Am. Chem. Soc. 2012, 134, 16773−16780

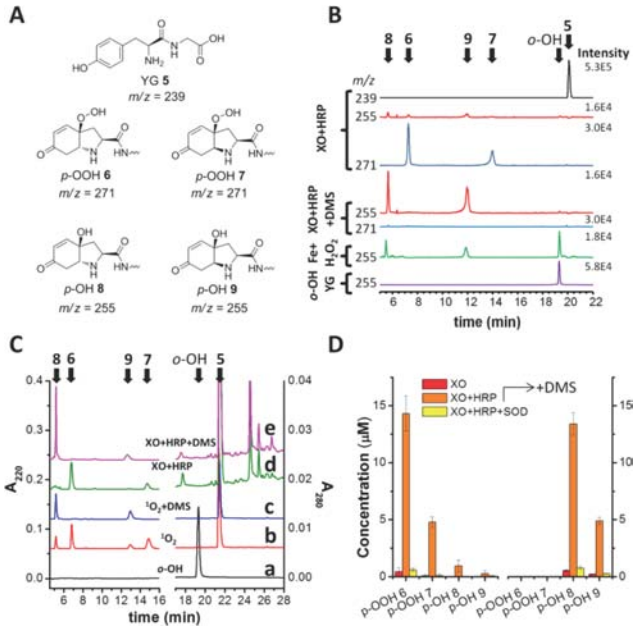

Figure 5. Oxidation of YG with XO and HRP. (A) Structures of YG and its derivatives. (B) Extracted ion chromatograms of YG exposed to different oxidizing systems. YG was incubated with XO, acetaldehyde, and HRP as described in Figure 2 (details in the Experimental section). The primary products consisted of *p*-OOH **6** and **7** (m/z = 271) that were reduced to alcohols *p*-OH **8** and **9** with DMS (m/z = 255) and that had the same retention time and fragmentation pattern as those produced by $^1O_2$ (not shown). No detectable amount of *o*-OH derivative was observed in this reaction by comparison with mushroom-tyrosinase generated standard. Hydroxylation by Fe(II):EDTA and hydrogen peroxide led to the formation of both *o*- and *p*-OH derivatives of YG. (C) RP-HPLC separation of the products of YG oxidation by XO and HRP monitored at 220 and 280 nm: (a) authentic *o*-OH YG derivative produced with mushroom tyrosinase; (b) YG oxidized with $^1O_2$, showing *p*-OOH **6** and **7** and *p*-OH **8** and **9**; (c) YG oxidized with $^1O_2$ and then reduced with DMS, showing *p*-OH **8** and **9**; (d) YG oxidized with XO and HRP; (e) YG oxidized with XO and HRP and then reduced with DMS. (D) Quantification of the different products showed that in the presence of both XO and HRP, *p*-OOH **6** was preferentially formed, followed by p-OOH **7**, which were converted stoichiometrically to *p*-OH **8** and **9** by reduction with DMS. No *o*-OH derivative was observed under these conditions. The formation of these products was reduced more than 20 times in the absence of HRP or after the addition of SOD, indicating the involvement of $O_2^{\bullet -}$ and tyrosyl radical in the formation of these products.

and **9**. Interestingly, hydroxylation of YG by Fe(II):EDTA and H_2O_2 produced both *o*- and *p*-OH derivatives, in contrast to tyrosinase that produced exclusively *o*-OH derivative (Figure 5B,C). The collision induced dissociation of YG **5** and its *o*-OH derivative showed a similar pattern, where the main fragments arose from the loss of NH_3 and the loss of the glycine and CO (Figure S1). In contrast, loss of H_2O was observed in both *p*-OH peaks, in addition to the loss of glycine and CO (Figure S1). The *p*-OOH derivatives showed a more complex fragmentation, involving loss of H_2O_2, in addition to the loss of H_2O, glycine, and CO (Figure S1).

Quantification of YG Oxidation Products. The major products from the addition of superoxide to the tyrosyl radical of YG, produced using XO and HRP, were *p*-OOH **6** and **7**, with only trace amounts of *p*-OH **8** and **9** (Figure 5D). Subsequent reduction with DMS completely converted *p*-OOH **6** and **7** to the alcohol derivatives *p*-OH **8** and **9**. No significant *o*-OH derivative of YG was observed under these conditions. The involvement of both $O_2^{\bullet -}$ and tyrosyl radical in the formation of these products is evidenced by the 20-fold decrease in the formation of *p*-OOH derivatives in the absence of HRP or in the presence of SOD (Figure 5D). The yield of *p*-OOH derivatives from YG **5** was 12 times higher than the one observed with GY **1**. This effect has been observed before and has been attributed to free amines favoring superoxide adduction rather than reduction to the N-terminal tyrosyl radical.[12,13,16,17]

NMR Structural Characterization of Products. Further characterization of the hydroxylated products by NMR confirmed that *p*-OH **8** and **9** were bicyclic indolic diastereoisomers (see in Tables S2 and S3). NOE NMR experiments enabled the assignment of configuration for *p*-OH **8** as (2*S*,3a*R*,7a*R*)-3a-hydroxy-6-oxo-2,3,3a,6,7,7a-hexahydro-1H-indole-2-carboxylic and *p*-OH **9** to (2*S*,3a*R*,7a*S*)-3a-hydroxy-6-oxo-2,3,3a,6,7,7a-hexahydro-1H-indole-2-carboxylic acid, respectively, as shown in Figure 6 (more details in Section

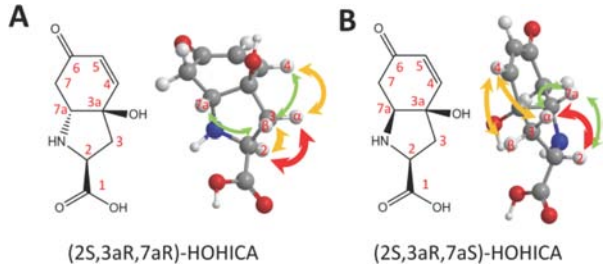

Figure 6. Stereochemistry of *p*-OH **8** and **9** assigned based on NOE NMR experiments. Key cross-peaks found in each diastereomer are shown by the arrows. The colors and thickness of the arrows indicate the strength of the NOE: red, strong; orange, medium; green, weak. (A) The oxidized tyrosine in *p*-OH **8** has the same configuration as (2*S*,3a*R*,7a*R*)-HOHICA: missing cross-peaks between H7a, H3α, and H2 indicates that H7a is in an opposite face to H2 and therefore should be 7a*R*. The difference in NOE between H3α and H3β to H4 indicates that is a *cis*-fused ring conformation and not a *trans*-fused ring, so it follows that 3a is *R* configuration. (B) The oxidized tyrosine in *p*-OH **9** has the same configuration as (2*S*,3a*R*,7a*S*)-HOHICA: observed cross-peaks between H7a, H3α, and H2 indicates they are on the same face of the molecule, that is 7a*S*. The similar NOE intensity between H3α and H3β to H4 suggests it is a *trans*-fused ring conformation, characteristic of 3a*R*,7a*S*. More detailed analysis and crude data are provided in Section S4, SI.

S4, SI). These structures are consistent with a Michael-type cyclization to give both *cis*- and *trans*-fused bicyclic products; the *cis*-fused *p*-OOH **6** being favored over the *trans*-fused *p*-OOH **7** by about 3:1. These bicyclic derivatives of tyrosine have the same core structure as HOHICA.[9,11] The stereochemical configurations determined here for the main product *p*-OH **8** are different from that originally reported by Jin et al.[11] but are in agreement with the recent report by Wright et al.[9]

LC-MS Analysis of Leu-Enkephalin Oxidation Products. Leu-enk oxidation by XO and HRP also led to the formation of bicyclic indolic compounds *p*-OOH **11** and **12** (m/z 588) and *p*-OH **13** and **14** (m/z 572) (Figure 7). No evidence for an *o*-OH derivative was found. Collision induced dissociation of all of the indolic compounds gave predominantly amide bond cleavage over side chain fragmentation. The mass shifts in b and y ions in the oxidation products of Leu-enk

dx.doi.org/10.1021/ja307215z | J. Am. Chem. Soc. 2012, 134, 16773−16780

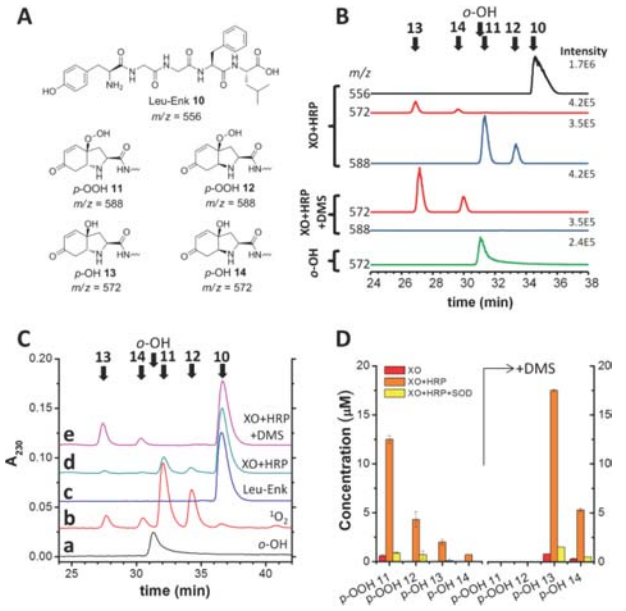

Figure 7. Oxidation of Leu-enk with XO and HRP. (A) Structures of Leu-enk and its derivatives. (B) Extracted ion chromatograms of Leu-enk exposed to different oxidizing systems. Leu-enk was incubated with XO, acetaldehyde, and HRP in order to generate superoxide and tyrosyl radical simultaneously (details in Figure 2). Both the hydroperoxide (m/z = 588) and the alcohol derivatives (m/z = 572) were monitored. The primary products consist of *p*-OOH **11** and **12** (m/z = 588) that were reduced to the alcohol derivatives *p*-OH **13** and **14** with DMS (m/z = 572). No *o*-OH derivative was observed in this reaction by comparison with authentic standard. (C) RP-HPLC chromatograms of Leu-enk oxidized with XO and HRP monitored at 230 nm: (a) authentic *o*-OH derivative of Leu-enk; (b) Leu-enk oxidized with $^1O_2$; (c) Leu-enk standard; (d) Leu-enk oxidized by XO and HRP; (e) Leu-enk oxidized by XO and HRP and then reduced with DMS. (D) Quantification of the different products showed that in the presence of both XO and HRP, *p*-OOH **11** was preferentially formed, followed by *p*-OOH **12**. Addition of DMS converted the *p*-OOH derivatives quantitatively to *p*-OH **13** and **14**. In the absence of HRP, or after adding SOD, the formation of these products was reduced more than 20 times, evidencing the involvement of superoxide and tyrosyl radical in the formation of the *p*- and *p*-OH derivatives.

indicated that the *p*-OOH and *p*-OH modifications are on the terminal tyrosine (Figure S2).

Quantification of Leu-Enkephalin Oxidation Products. When Leu-enk was oxidized with XO and HRP, the *p*-OOH derivatives **11** and **12** predominated, being approximately six times more abundant than the corresponding *p*-OH derivatives **13** and **14** (Figure 7D). After treatment with DMS, both *p*-OOH compounds were reduced to the *p*-OH derivatives quantitatively, with a product ratio of 3:1 *p*-OH **13**:**14**.

NMR Structural Characterization. The structures of *p*-OH **13** and **14** were confirmed by ^{1}H, COSY, HSQC, HMBC, and NOE NMR experiments (Tables S4 and S5). The two diastereomeric *p*-OH **13** and **14** compounds did not show much difference in ^{1}H NMR (Table S5). Distinctive differences found in NOE indicated that *p*-OH **13** had a *cis*-fused ring conformation, while *p*-OH **14** had the *trans*-fused ring (see a detailed explanation in in Section S4, SI). As was the case for YG, the nucleophilic addition for Leu-enk favors the *cis*-fused bicyclic system in a ratio of 3:1 *p*-OOH **11**:**12**.

***p*-Hydroxylation by Hydroxyl Radical.** Exposing the peptides to hydroxyl radical generated from Fe(II):EDTA-catalyzed decomposition of H_2O_2 led to hydroxylation at both *ortho* and *para* positions of tyrosine. The formation of GY and YG *p*-OH derivatives is evident by LC-MS matching m/z = 255 and retention time with the same fragmentation patterns as those generated by $^1O_2$ or XO/HRP oxidation (Figures 2 and 5). No hydroperoxide derivatives were observed under these conditions. Quantification of the hydroxylated products showed that *para* hydroxylation was a minor process relative to *ortho* hydroxylation: *p*-OH **3** accounted for 12% relative *o*-OH **4** and *p*-OH **9** accounted for 6% relative to the *o*-OH derivative (Table 1).

Table 1. *o*- and *p*-Hydroxylation of Tyrosine in GY and YG by Fenton-Generated Hydroxyl Radical[a]

	products	concentration (μM)
GY	*o*-OH **4**	30 ± 3
	p−OH **3**	3.8 ± 0.3
YG	*o*-OH	12.7 ± 0.9
	p−OH **9**	0.8 ± 0.1

[a]2.0 mM GY or YG exposed to 0.4 mM $FeSO_4$, 0.8 mM EDTA, and 0.4 mM H_2O_2 in 5 mM sodium phosphate at pH 7.4 for 5 min at room temperature. Sample was then acidified to 0.2 M HCl and analyzed by HPLC-UV. Experiments were done in triplicate, and results are expressed as mean ± SD.

Little oxidation of Leu-enk occurred under the Fenton conditions used for reaction of GY and YG, but when Leu-enk was reacted with 10-fold more H_2O_2 and Fe(II):EDTA, oxidation products were observed by LC-MS. At least five different peaks with an m/z consistent with the addition of one atom of oxygen were found (m/z = 572, Figure S3). According to their fragmentation patterns, the peaks 1 and 2 were identified as phenylalanine hydroxylation products (Figure S4). Peaks 3−5 had the same retention time and fragmentation pattern as those of *p*-OH **13** and **14** and the *o*-OH derivative (Figures S3−S5). We also found a hydroperoxide on the leucine (m/z = 588), based on the shifts in b and y ions (Figure S5). Leucine hydroperoxides have been observed before in proteins exposed to peroxyl and alkoxy radicals.[23]

DISCUSSION

Superoxide and tyrosyl radicals are two of the most abundant free radicals in biology. Superoxide can be produced by many pathways including its direct formation by the enzymes NADPH oxidase and xanthine oxidase and as a result of electron leakage in the mitochondrial electron transport chain. Furthermore, many pathological conditions including diabetes, cardiovascular disease, and cancer are associated with an increased production of superoxide from these sources.[24−26]

The tyrosyl radical can also be formed by multiple pathways, including oxidation of tyrosine by oxygen radicals, nitrogen dioxide, carbonate radical, and hemeperoxidases.[1,2,27−29] *o*-Nitrotyrosine and *o*,*o*′-dityrosine are detected *in vivo* in normal conditions and are usually increased in pathological conditions, providing evidence of tyrosyl radical formation *in vivo*.[1,28−31] The reaction between superoxide and tyrosyl radicals occurs at nearly diffusion-controlled rates ($k = 1.5 \times 10^9$ M^{-1} s^{-1}),[11,16] suggesting that this reaction may be important *in vivo*. There are a large number of alternative possible reactions for these radicals *in vivo* that will affect the amount of *p*-OOH formed. Lancaster built a kinetic model that takes into account the most important reactions of oxygen and nitrogen reactive species

dx.doi.org/10.1021/ja307215z | J. Am. Chem. Soc. 2012, 134, 16773−16780

with other radicals and low molecular weight and enzymatic antioxidants under biological conditions.[32] One of the conclusions of this work was that the main reactions of tyrosyl radical were the radical swap with glutathione and the reaction with superoxide, the latter being significantly more important than the reaction with nitrogen dioxide.[32] All these results suggest that *p*-OOH and *p*-OH derivatives of tyrosine should be significantly more abundant than *o*-nitrotyrosine. We are presently developing methods to quantify *p*-OH-tyr to clarify this matter.

In most of the recent work on superoxide addition to tyrosyl radicals the *ortho*−*para* selectivity of adduction was not addressed and the structure of products formed was left unresolved.[12,14−18] Our results demonstrate that tyrosyl radicals of different peptides react with superoxide to produce hydroperoxides predominately in the *para* position of tyrosine. This conclusion was evident by LC-MS and HPLC-UV when the products of XO/HRP oxidation were compared to the *o*-OH products generated from enzymatic oxidation with mushroom tyrosinase and to the *p*-OH and *p*-OOH products generated from singlet oxygen. Furthermore, reduction of the XO/HRP or singlet oxygen-derived hydroperoxides with DMS led exclusively to the *p*-OH derivatives, confirmed by LC-MS, HPLC-UV, and NMR. In contrast, the dopa-like *o*-OH tyrosine derivatives could only be observed in very low amounts from GY, and these products were unaffected by DMS, indicating that no stable hydroperoxides are precursors to these compounds.

In the case of YG and Leu-enk, where the tyrosine is N-terminal, the oxidized tyrosine formed a bicyclic indolic alcohol (HOHICA) after reduction with DMS. Hydroperoxides were not studied directly by NMR, but their reduction with DMS led to a single alcohol derivative, indicating that the formation of the bicyclic structure occurred at the hydroperoxide stage. Two major diasteroisomers were observed in both YG and Leu-enk, that were assigned to two different configurations of HOHICA, the *cis*-fused ring 2*S*,3a*R*,7a*R* and the *trans*-fused ring 2*S*,3a*R*,7a*S* (Figure 7). These bicyclic structures are formed by amine conjugate attack to the α,β-carbonyl of the intermediate noncyclized cyclohexadienone *p*-OOH, and the addition occurs preferentially from the face of the ring opposite to the hydroperoxide, giving the *cis*-fused ring 2*S*,3a*R*,7a*R* compound as the major product.

In the case of GY, where the tyrosyl is C-terminal, the *p*-OH derivative (**3**) did not undergo cyclization. Other peptides with N-protected tyrosine, such as N-acetyl-Tyr-Ala methyl ester,[8] [Tyr5]bradykinin (to be published), and Gly-Tyr-Gly,[9] formed stable *p*-OH products after oxidation, suggesting that cyclization occurs readily only in N-terminal tyrosine containing peptides.

The selective addition of superoxide to the *para* position of tyrosyl radicals is intriguing. In the tyrosyl radical both the *ortho* and the *para* positions are spin-rich, and the *ortho* site is preferred for the addition of many radicals, including nitrogen dioxide and a second tyrosyl.[1,17,28,30] There are of course two available *ortho* positions, which are less sterically hindered than the one *para* site, and the addition of radicals ortho allows ultimately for rearomatization. Quantum calculations indicate that the formation of the product of addition of superoxide to tyrosyl radical in the *ortho* position is thermodynamically more favorable over the reaction at the *para* position.[17] The same study showed that the charge distribution in the tyrosyl radical placed a significant negative charge at the *ortho* positions,[17] and this could explain the experimentally observed preference for the *para* position: The negative charge at the *ortho* positions is acting as a kinetic barrier that slows down the reaction with the negatively charged superoxide at that site.

The N-terminal tyrosine peptides studied here gave 10-fold more superoxide adduction under identical reaction conditions than those peptides having an internal tyrosine. This propensity for N-terminal tyrosines to give more oxidation products in reactions with XO/HRP has been observed before and has been attributed the selective preference for adduction rather than reduction of superoxide to the N-terminal tyrosyl radical.[12,13,16,17]

The reaction of YG and GY under Fenton conditions shown in Table 1 confirm earlier reports that tyrosine hydroxylation by hydroxyl radical from different sources gives dopa-like *o*-OH derivatives as the main products.[33−36] The work by Solar et al. on the reaction of $^{\bullet}$OH with tyrosine by pulse radiolysis suggested indirectly that *para* and *ipso* addition of $^{\bullet}$OH were formed, but no products were isolated and characterized.[37] Hydroxyl radical has been shown to give approximately 10% of the *p*-OH product in its reaction with *p*-cresol,[38,39] but our studies with YG and GY appear to be the first time that *p*-OH products have been unambiguously shown to be a part of the Fenton-tyrosine product mixture.

Recent studies identified 64 endogenous sites of tyrosine hydroxylation in rat brain and heart proteins, most of which locate in the mitochondria,[6] and 9 endogenous sites of tyrosine hydroxylation in human cells (HeLa) mitochondria.[40] Taking into account the many ways through which *p*-OH derivatives of tyrosine can be generated and that these *p*-OH derivatives ionize better by electrospray than dopa-like derivatives, it is very likely that some of the identified sites of hydroxylation correspond to *p*-OH derivatives, rather than the assigned *o*-OH.[6,40] Caution is recommended when interpreting endogenous tyrosine hydroxylation, and *p*-OH tyrosine should be considered as an additional relevant product.

There are at least four routes that generate *para*-substituted tyrosines: (1) the reaction between tyrosyl radical and lipid peroxyl radicals;[8] (2) the reaction between tyrosyl radical and superoxide; (3) the hydroxylation of tyrosine via hydroxyl radical (presented here); and (4) the reaction of tyrosine with $^1O_2$. These *para*-substituted tyrosines are powerful electrophiles and can form adducts with thiols and other nucleophiles. Using peptides having tyrosines at sites other than the N-terminus, we observed the formation of Michael-type adducts with a number of nucleophiles of biological interest, including the addition of two cysteines to a single oxidized tyrosine (manuscript in preparation). While preparing this manuscript, a report by Nagy et al. appeared that showed that N-terminal tyrosine-containing peptides formed monoadducts with glutathione when oxidized with XO and HRP.[18] It seems clear from our work that the products reported are the result of tyrosine *para* oxidation and Michael addition to the indolic bicycles. It also follows that N-terminal tyrosines will give adduction of only one nucleophile while oxidation of tyrosines at sites other than the N-terminus can lead to mono- or diadduction of nucleophiles (see Scheme 2 for an example of adduction of two thiol nucleophiles) with potentially important biological consequences. As has been observed for other electrophiles, such as 4-hydroxynonenal, it is possible that at low concentrations these electrophilic *para*-substituted tyrosines trigger adaptive responses, like heat shock response or antioxidant response to prevent further damage.[41,42] On the

Scheme 2

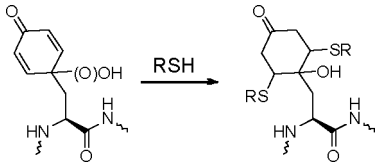

other hand, higher concentrations of these modified tyrosines could contribute to protein aggregation, such as that associated with neurodegenerative diseases,[43,44] promote cellular damage, and ultimately lead to cell death. Such potential biological roles warrant further investigation of these tyrosine-derived electrophiles.

CONCLUSIONS

The reaction between tyrosyl radicals and superoxide yields *para*-hydroperoxide derivatives that can cyclize to mostly a cis-fused indolic derivative, 2*S*,3a*R*,7a*R*-HOHICA, when the tyrosine is N-terminal, or remain as an acyclic *p*-OOH cyclohexadienone when the tyrosine is elsewhere in the peptide. The hydroperoxide can hydrolyze spontaneously or be reduced to yield the corresponding *p*-alcohol. Both products contain α,β-unsaturated carbonyls, which make them good electrophiles, and could confer on them interesting biological properties. We are presently assessing the formation of these electrophilic tyrosine-derivatives *in vivo* as well as their biological effects.

ASSOCIATED CONTENT

Supporting Information

Tables of ^{1}H and ^{13}C NMR chemical shifts, 1D and 2D NMR spectra, HPLC-MS data, and mass spectra of all the compounds. This material is available free of charge via the Internet at http://pubs.acs.org.

AUTHOR INFORMATION

Corresponding Author

n.porter@vanderbilt.edu

Notes

The authors declare no competing financial interest.

ACKNOWLEDGMENTS

N.P. thanks the National Science Foundation for support of this work. We thank Professor Rafael Radi from the Universidad de la República, Montevideo, Uruguay, Yoel García-Díaz of Vanderbilt University for helpful discussions, and Donald Stec for assistance in NMR experiments.

REFERENCES

(1) Radi, R. *Proc. Natl. Acad. Sci. U.S.A.* **2004**, *101*, 4003.
(2) Ischiropoulos, H. *Arch. Biochem. Biophys.* **1998**, *356*, 1.
(3) Ischiropoulos, H. *Arch. Biochem. Biophys.* **2009**, *484*, 117.
(4) Shao, B.; Oda, M. N.; Oram, J. F.; Heinecke, J. W. *Chem. Res. Toxicol.* **2010**, *23*, 447.
(5) Pennathur, S.; Wagner, J. D.; Leeuwenburgh, C.; Litwak, K. N.; Heinecke, J. W. *J. Clin. Invest.* **2001**, *107*, 853.
(6) Zhang, X.; Monroe, M. E.; Chen, B.; Chin, M. H.; Heibeck, T. H.; Schepmoes, A. A.; Yang, F.; Petritis, B. O.; Camp, D. G., 2nd; Pounds, J. G.; Jacobs, J. M.; Smith, D. J.; Bigelow, D. J.; Smith, R. D.; Qian, W. J. *Mol. Cell. Proteomics* **2010**, *9*, 1199.
(7) Fu, S.; Davies, M. J.; Stocker, R.; Dean, R. T. *Biochem. J.* **1998**, 333 (Pt 3), 519.
(8) Shchepin, R.; Möller, M. N.; Kim, H. Y.; Hatch, D. M.; Bartesaghi, S.; Kalyanaraman, B.; Radi, R.; Porter, N. A. *J. Am. Chem. Soc.* **2010**, *132*, 17490.
(9) Wright, A.; Bubb, W. A.; Hawkins, C. L.; Davies, M. J. *Photochem. Photobiol.* **2002**, *76*, 35.
(10) Jin, F.; Leitich, J.; von Sonntag, C. *J. Photochem. Photobiol A* **1995**, *92*, 147.
(11) Jin, F.; Leitich, J.; von Sonntag, C. *J. Chem. Soc., Perkin Trans.* **1993**, *2*, 1583.
(12) Nagy, P.; Kettle, A. J.; Winterbourn, C. C. *J. Biol. Chem.* **2009**, *284*, 14723.
(13) Winterbourn, C. C.; Parsons-Mair, H. N.; Gebicki, S.; Gebicki, J. M.; Davies, M. J. *Biochem. J.* **2004**, *381*, 241.
(14) Nagy, P.; Kettle, A. J.; Winterbourn, C. C. *Free Radical Biol. Med.* **2010**, *49*, 792.
(15) Das, A. B.; Nagy, P.; Abbott, H. F.; Winterbourn, C. C.; Kettle, A. J. *Free Radical Biol. Med.* **2010**, *48*, 1540.
(16) Mozziconacci, O.; Mirkowski, J.; Rusconi, F.; Pernot, P.; Bobrowski, K.; Houee-Levin, C. *Free Radical Biol. Med.* **2007**, *43*, 229.
(17) Field, S. M.; Villamena, F. A. *Chem. Res. Toxicol.* **2008**, *21*, 1923.
(18) Nagy, P.; Lechte, T. P.; Das, A. B.; Winterbourn, C. C. *J. Biol. Chem.* **2012**, *287*, 26068.
(19) Edelhoch, H. *Biochemistry* **1967**, *6*, 1948.
(20) Marumo, K.; Waite, J. H. *Biochim. Biophys. Acta* **1986**, *872*, 98.
(21) Buettner, G. R. *Arch. Biochem. Biophys.* **1993**, *300*, 535.
(22) Folkes, L. K.; Trujillo, M.; Bartesaghi, S.; Radi, R.; Wardman, P. *Arch. Biochem. Biophys.* **2011**, *506*, 242.
(23) Steinmann, D.; Ji, J. A.; Wang, Y. J.; Schoneich, C. *Mol. Pharm.* **2012**, *9*, 803.
(24) Guzik, T. J.; Mussa, S.; Gastaldi, D.; Sadowski, J.; Ratnatunga, C.; Pillai, R.; Channon, K. M. *Circulation* **2002**, *105*, 1656.
(25) Kelkar, A.; Kuo, A.; Frishman, W. H. *Cardiol. Rev.* **2011**, *19*, 265.
(26) Dikalov, S. *Free Radical Biol. Med.* **2011**, *51*, 1289.
(27) Augusto, O.; Bonini, M. G.; Amanso, A. M.; Linares, E.; Santos, C. C.; De Menezes, S. L. *Free Radical Biol. Med.* **2002**, *32*, 841.
(28) Heinecke, J. W.; Li, W.; Francis, G. A.; Goldstein, J. A. *J. Clin. Invest.* **1993**, *91*, 2866.
(29) Heinecke, J. W.; Li, W.; Daehnke, H. L., III; Goldstein, J. A. *J. Biol. Chem.* **1993**, *268*, 4069.
(30) DiMarco, T.; Giulivi, C. *Mass Spectrom. Rev.* **2007**, *26*, 108.
(31) Pennathur, S.; Bergt, C.; Shao, B.; Byun, J.; Kassim, S. Y.; Singh, P.; Green, P. S.; McDonald, T. O.; Brunzell, J.; Chait, A.; Oram, J. F.; O'Brien, K.; Geary, R. L.; Heinecke, J. W. *J. Biol. Chem.* **2004**, *279*, 42977.
(32) Lancaster, J. R., Jr. *Chem. Res. Toxicol.* **2006**, *19*, 1160.
(33) Lynn, K.; Purdie, J. *Int. J. Radiat. Phys. Chem.* **1976**, *8*, 685.
(34) Boguta, G.; Dancewicz, A. *Int. J. Radiat. Biol.* **1981**, *39*, 163.
(35) Getoff, N. *Amino Acids* **1992**, *2*, 195.
(36) Maskos, Z.; Rush, J. D.; Koppenol, W. H. *Arch. Biochem. Biophys.* **1992**, *296*, 521.
(37) Solar, S.; Solar, W.; Getoff, N. *J. Phys. Chem.* **1984**, *88*, 2091.
(38) Schuler, R. H.; Albarran, G.; Zajicek, J.; George, M. V.; Fessenden, R. W.; Carmichael, I. *J. Phys. Chem. A* **2002**, *106*, 12178.
(39) Albarran, G.; Schuler, R. H. *J. Phys. Chem. A* **2005**, *109*, 9363.
(40) Lee, S.; Chen, Y.; Luo, H.; Wu, A. A.; Wilde, M.; Schumacker, P. T.; Zhao, Y. *J. Proteome Res.* **2010**, *9*, 5705.
(41) Jacobs, A. T.; Marnett, L. J. *Acc. Chem. Res.* **2010**, *43*, 673.
(42) Iles, K. E.; Dickinson, D. A.; Wigley, A. F.; Welty, N. E.; Blank, V.; Forman, H. J. *Free Radical Biol. Med.* **2005**, *39*, 355.
(43) Giasson, B. I.; Duda, J. E.; Murray, I. V.; Chen, Q.; Souza, J. M.; Hurtig, H. I.; Ischiropoulos, H.; Trojanowski, J. Q.; Lee, V. M. *Science* **2000**, *290*, 985.
(44) Stefani, M.; Dobson, C. M. *J. Mol. Med. (Berl)* **2003**, *81*, 678.